EUROPEAN ORGANIZATION FOR NUCLEAR RESEARCH
ORGANISATION EUROPEENNE POUR LA RECHERCHE NUCLEAIRE

CERN - PS DIVISION

PS/ PA/ Note 95-24

Magnetic Measurements on PIS MH 42 Lead Ion

J. Borburgh

Geneva, Switzerland
12 October 1995

1. Introduction

Before installation in the PS complex it was necessary to test the magnets at various currents corresponding to the various beam energies required. Tests were carried out to perform magnetic measurements and compare with the calculated design values at different current levels. The results of these tests are tabulated in this report.

Figure 1 shows the equivalent circuit diagram is shown and the place where induction measurements were made. In figure 2 the positions are indicated where the different magnetic measurements were taken.

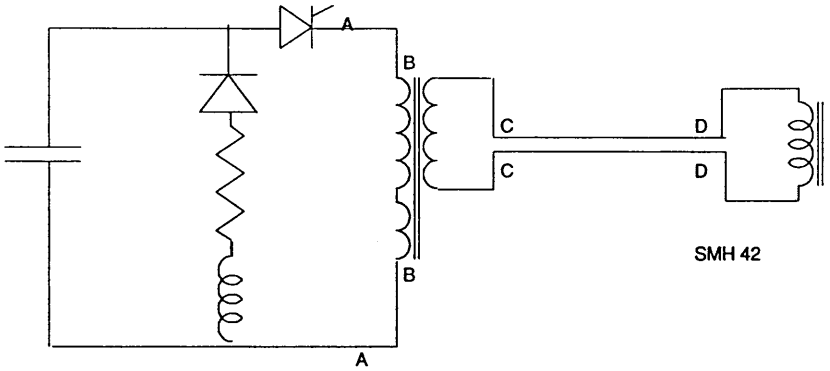

Figure 1: the circuit diagram

The equivalent circuit specifications were:

Capacitance	3 mF
Transformer	12 : 1

The measuring equipment used was:

Impedance meter	H.P. Model and Philips Fluke PM
Current Transformer	Pearson Model 1423 (1 V/kA)
Digitiser	Tektronix 7612D
Data handling	486 p.c. with Labview
Scope	H.P. Model 54601 A

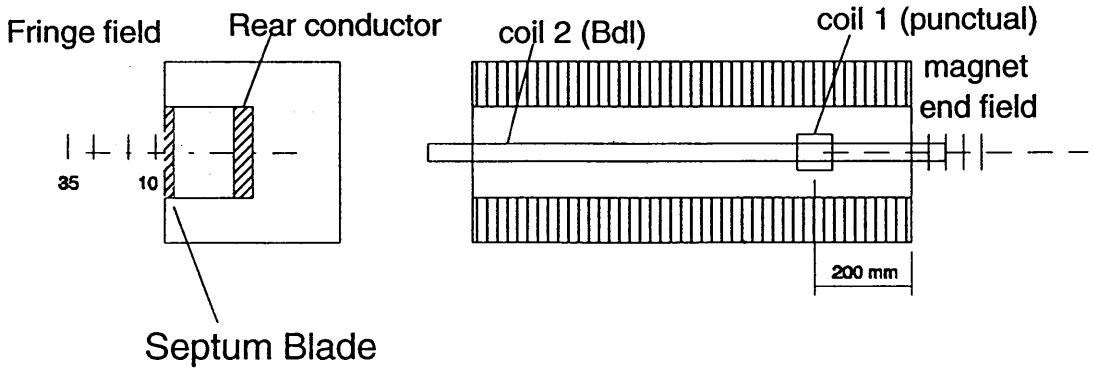

Figure 2: magnetic measurement positions

2. Inductance measurements

The inductance of the magnet itself was calculated at 1.27 μH for a quasi dc situation. Using an impedance meter the individual values of resistance and inductance off the discharge circuit were measured at two frequencies. By bridging the circuit at point D (see figure 1) the inductance as seen by the primary of the power supply (point A, figure 1) can be determined. In table 1 the results are reproduced.

Table 1 : inductance measurements on magnet PISMH 42.2

Inductance	L(μH)	L(μH)
Frequency	1 kHz	120 Hz
Short circuit @ D	102	112
No short circuit	303	328
Derived magnet inductance	**1.39**	**1.50**

The magnet PISMH 42.1 is build exactly the same, so it was assumed that the inductance does not differ much from on magnet to another. Therefore no measurement was taken on magnet PISMH 42.1. The values measured on PISMH 42.2 are close to the values calculated. The difference can be explained by the connection between the magnet and the outside world (feedthrough), which is not taken into account for the theoretical i.e. calculated value. Since the old magnet was a twelve turn DC magnet, these new magnets have a much lower inductance.

3. Current Characteristics

The septum magnets were connected to the power supply as shown in figure 1 of this report. The capacitor bank was 3 mF. The current wave form was measured for magnet SMH42.2. Three characteristic quantities can be defined:

-I_{top}, the top value of the current
-T_{top}, time from start until I_{top} occurs
-$T_{\frac{1}{2}\omega}$, the length of the half sine

These quantities are tabulated in table 2 and the current waveform itself is shown in figure 3.

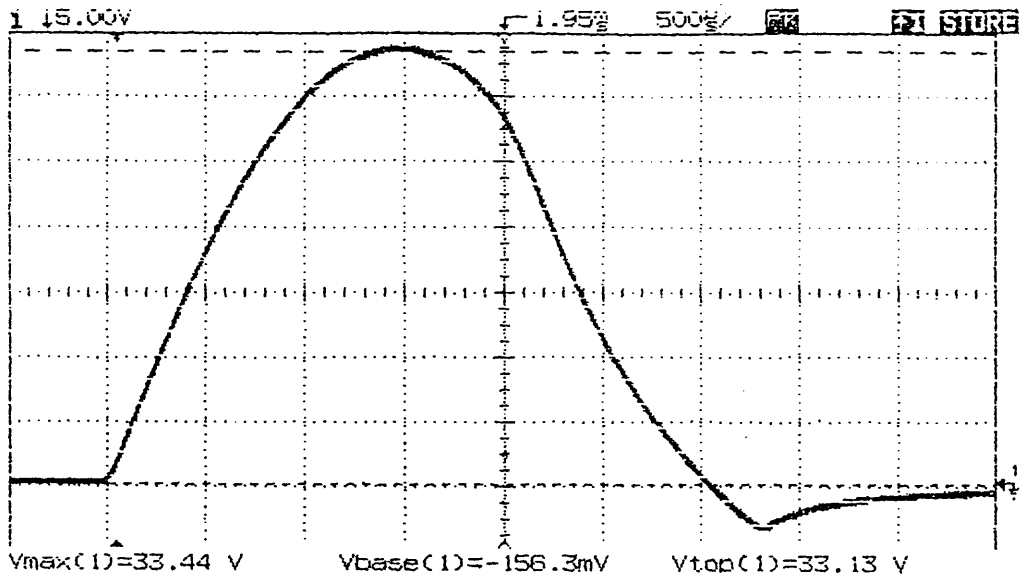

Figure 3: current waveform of PISMH 42.2 at 33.5 kA

Table 2: T_{top} and $T_{\P/\omega}$ for different currents of the magnet

I_{top} (kA)	$T_{\P/\omega}$ (ms)	T_{top} (ms)	with an deflection angle of 54.7 mrad this current corresponds with:
12.5	3.40	1.42	0.8 GeV/c
15.6	3.37	1.42	1.0 GeV/c
21.9	3.36	1.43	1.4 GeV/c
22.9	3.32	1.49	0.8 GeV
26.5	3.32	1.49	1.0 GeV
33.5	3.02	1.49	1.4 GeV

4. Magnetic measurements

Using the power supply described previously with a pulse repetition rate of approximately 4.5 seconds a series of measurements were recorded in order to determine the magnetic field in the gap, the fringe field, close to the septum, and the end. The field in the gap was measured to determine the actual punctual values and also the Bdl from which we can calculate the equivalent magnetic length of the magnet. Two types of measuring coils were used and their characteristics are given below.

a. For punctual field values,

Coil 1; surface area = 0.03693m^2 ; ($\varnothing$ = 5 mm)^2

b. For Bdl measurements,

Coil 2; specific surface=0.05763 m^2/m; (Surface area = 0.0750m^2, length 1.30 m)

With the small measuring coil (coil 1) the field was measured in the middle of the gap and at one third of the length of the septum. With the program 'B measurementv311' running under Labview, the fields were measured. This program is described in note PS/PA 95-13.

4.1 Measurements inside the magnet gap

In this paragraph tables and diagrams are shown of the field in the gap, measured with coil 1, and the integrated field through the gap measured over more than the full length of the magnet to obtain the equivalent length of the magnet. The results for magnet SMH42.2 are shown in table 3 and figures 4a and 4b.
The same measurements were made with magnet SMH42.1 in order to make a comparison between the two physically identical magnets to verify that no serious deviations occurred from one magnet to the other. These results are shown in table 4 as well as in figures 4a and 4b.

Table 3: Magnetic measurements inside the gap of SMH42.2

Magnet current (kA)	Bdl (mT.m)	Bo (T)	L equiv. (mm)
12.5	148	0.260	569
15.6	184	0.324	569
21.9	259	0.454	570
22.9	270	0.476	568
26.5	314	0.552	569
33.5	395	0.697	567
39	460	0.815	564

Table 4: Magnetic measurements inside the gap of SMH42.1

Iseptum (kA)	Bdl (mT.m)	B_0 (T)	L equiv. (mm)
12.5	146	0.256	568
15.6	183	0.322	568
21.9	256	0.451	569
22.9	268	0.472	569
26.5	312	0.549	567
33.5	397	0.701	566
39	462	0.818	565

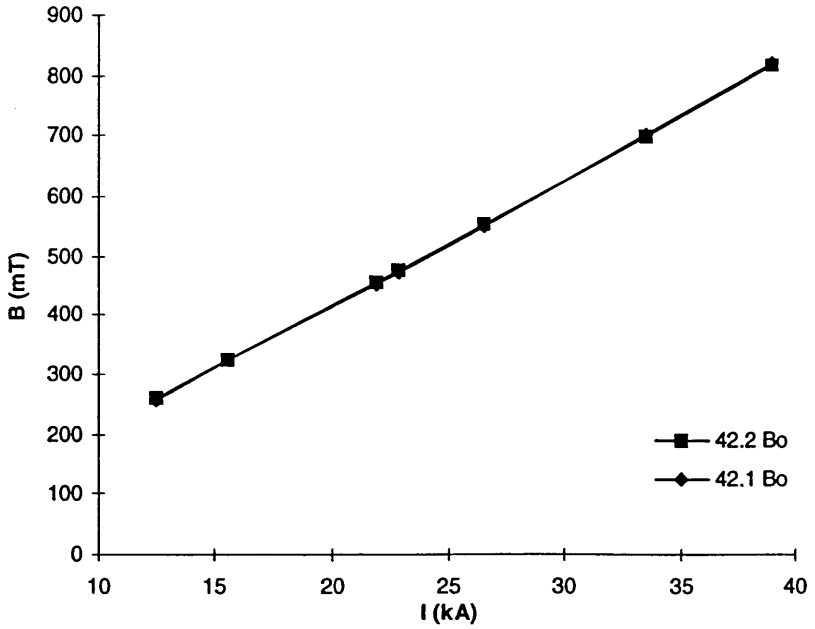

Figure 4a: B_0 measurement in the gap

What can be noticed is, that no measurable saturation occurs, even for very large currents. Also the differences in field strength between the magnets is negligible.

Also the equivalent length (L_{equiv}) is tabulated in table 3 and 4. This length is calculated by dividing the integrated field by the corresponding field strength. This length is equivalent to the length of a theoretical magnet with field strength B_0 and no field outside the magnet. The tables show there is little variation in L_{equiv}, what indicates there

is no saturation. The expected equivalent magnetic length is 560 mm and the measured length is within acceptable tolerance of this expectation.

For estimation of the equivalent length a good rule of thumb appears to be to take the distance of the septum between the cross over conductors and add two times half the width of these cross over conductors. In the case of this magnet this adds up to 547mm + 2 times 9 mm = 565 mm. This is within 1 % of what has been measured.

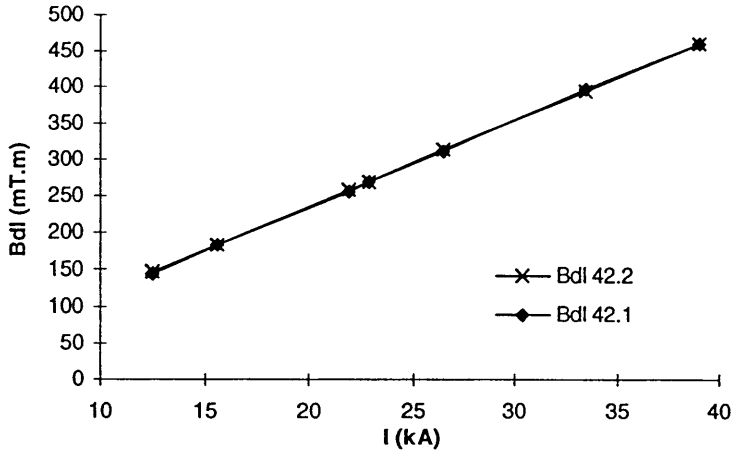

Figure 4b: Bdl measurements in the gap

4.2 Measurement of the fringe field next to the septum

Measurements were carried out to determine the magnitude of the integrated fringe field parallel and close to the septum blade in order to assess the effect on the orbiting beam. The results were taken at several separate distances from the septum with results presented in table 5a and 5b. These results are graphically shown in figure 5.

Table 5a: Fringe field measurements on SMH42.2

Distance from septum blade (mm)	Bdl (mT.m) (at 26.5 kA)	Bdl (mT.m) (at 33.5 kA)
10	2.120	2.763
15	1.440	1.873
25	0.749	0.968
35	0.454	0.575
45	0.286	0.460
55	0.194	0.410
65	0.145	0.369

Table 5b: Fringe field measurements on SMH42.1

Distance from septum blade (mm)	Bdl (mT.m) (at 26.5 kA)	Bdl (mT.m) (at 33.5 kA)
5	2.769	3.639
10	2.053	2.614
15	1.425	1.805
25	0.710	0.949
35	0.410	0.627
45	0.266	0.462
55	0.171	0.463

The stray field next to the magnet SMH42.2 is slightly larger than the stray field of magnet SMH42.1, approximately 3 %. This is due to building tolerances of the magnets. The absolute values however of the stray fields are low enough not to affect the circulating beam.

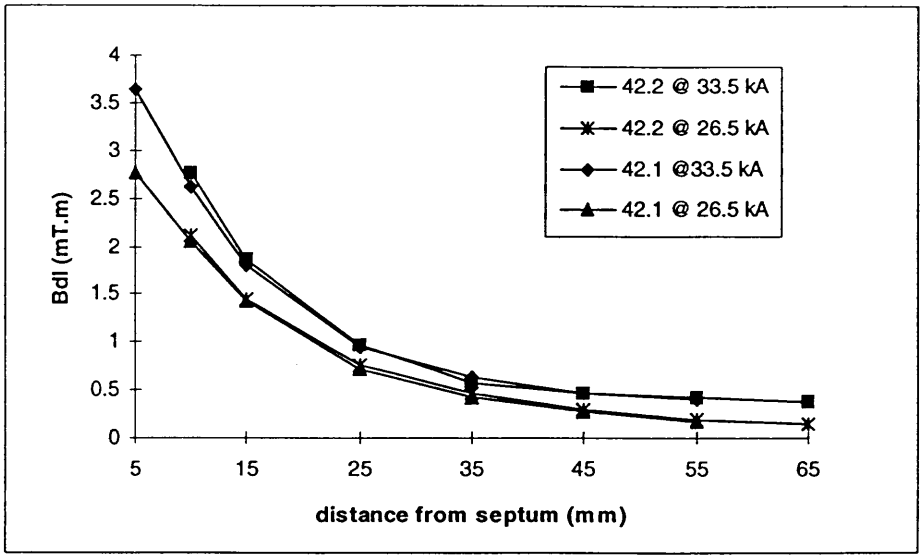

Figure 5: Integrated fringe field measurements

4.3 Measurement of the leakage field at the end of the magnet

The field was measured at several positions in front of the middle of the magnet gap to determine the magnitude of the end field due to leakage. The measurements have been taken for two different currents. The results are shown in tables 6a and 6b, and illustrated in figure 6.

Table 6a: End field for SMH42.1

position (mm)	B (mT) (26.5 kA)	B (mT) (33.5 kA)
0	41.9	52.8
10	22.6	28.9
20	12.8	17.2
30	8.09	10.7
40	5.37	7.22
50	3.68	4.92
60	2.58	3.43

Table 6b: End field for SMH42.2

position (mm)	B (mT) (26.5 kA)	B (mT) (33.5 kA)
0	31.2	41.6
10	17.3	23.3
20	10.5	14.1
30	6.57	9.22
40	4.45	6.13
50	3.21	4.23
60	2.23	2.95

What can be seen in figure 6 is that the end fields drop very rapidly, as can be expected. This field also contributes to the magnetic length of the magnet. The measurements of the two different magnets seem not to be consistent. An explanation for the differences might be a misalignment of the measurement coil for the PISMH42.2.

Another reason for measuring these fields is that there are two SEM wire frames attached at the end of the magnets. The end field may disturb these beam observation systems. The two SEM wire frames are at 17 and 41 mm from the endplate, while the inner wall of the vacuum tank is at 56 mm from the endplate.

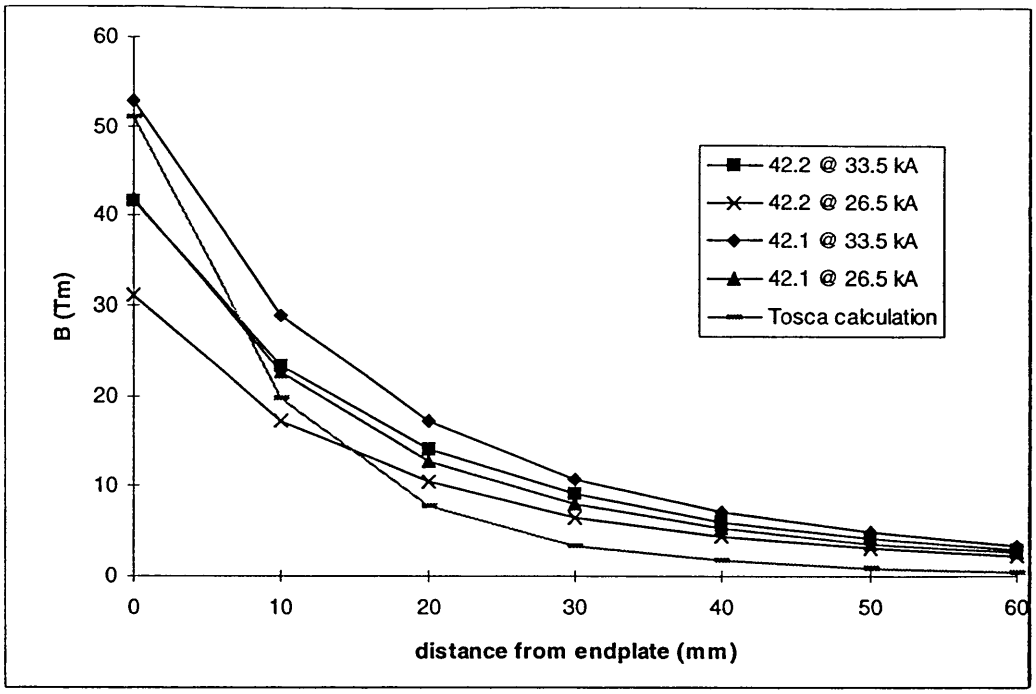

Figure 6: End field decay as measured from the outside of the endplate

5. Conclusions

The inductance measurements have shown that the measured values for the new magnets are within 1% of the calculated ones.

The current wave forms are measured and are as can be expected.

Leakage fields at the ends of the new magnet are as expected, because the equivalent length of the magnet measured is close to the equivalent length expected from the calculations. The stray field next to the septum blade of the new magnets is low, lower then 1% of the gap field at 10 mm from the septum, and lower then 1/1000 at 50 mm distance from the septum.

A good rule of thumb has been found for the estimation of the equivalent length of a elektromagnetic septum magnet. The equivalent length is approximately the length of the septum blade between the cross over conductors plus the width of one cross over conductor. This rule proved to be within 1 % of the measured value of the equivalent length.

The cooling requirements are were difficult to measure, since the variations in temperature seen at the outlet of the magnet, were in the same range as the variations of the inlet temperature during the test, i.e. 4 °C.

COMPARISON between OLD and NEW SMH42

J. Borburgh

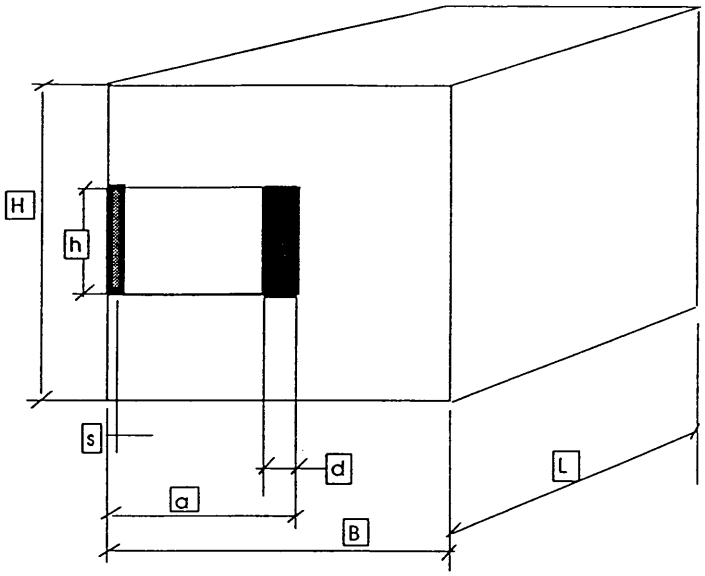

all dimensions in mm

		old SMH42	**new SMH42**
Laminations			
gap			
	h	*60.4*	**60.4**
	a	*120*	**116**
	s	*5*	**5**
	d	*15*	**8.8**
external			
	B	*200*	**195**
	H	*180*	**200**
	L total	*700*	**610**
	L equivalent	*640*	**560**

Electrical and magnetic characteristics

Protons, 0.8 GeV	**deflection = 54.66 mrad**			
	int. B.dl	*0.27*	**0.27**	T.m
	Bo	*0.416*	**0.476**	T
	Current	*1.665*	**22.9**	kA
Protons, 1.0 GeV	**deflection = 54.66 mrad**			
	int. B.dl	*0.309*	**0.309**	T.m
	Bo	*0.482*	**0.552**	T
	Current	*1.931*	**26.5**	kA
Protons 1.4 GeV	**deflection = 54.66 mrad**			
	int. B.dl		**0.39**	T.m
	Bo		**0.697**	T
	Current		**33.5**	kA

M.THIVENT Version 12 Mai 1992 Edition du : 30.Jun.95
Modifie R, L pour monospire, hydraulique revise 2/8/94 J. Borburgh

PREDETERMINATION SEPTUM MAGNETIQUE SMCALC.XLS **PW prot:jb**

PISMH 42 version ION PLOMB

particularités

DONNEES			RESULTATS PROTONS		
particules electrons : e protons : p	p		Masse au repos mo	0.94	Gev/c2
quant.mouvt : MV Energie cin. : EC	ec		**Energie cinétique**	**1.4000**	GeV
			Quantité de mouvement	**2.1429**	Gev/c
Energie cinétique Ec =	1.4	GeV	beta	0.9158	
			gamma	2.4894	
Déflexion requise	54.66	mrad	beta*gamma	2.2797	
Epaisseur du septum	5	mm	Déplact. après espace de gliss	15.3048	mm
Hauteur du Gap	60.4	mm			
Profondeur du Gap	116	mm	**Champ intégré B*L**	**0.390**	T.m
Longueur magnetique equivalent	560	mm	**Induction dans le Gap**	**0.697**	T
Espace de glissement	0	m	Champ magn. H=B/uo	5.55E+05	A/m
Monospire donc	1	spire	**Courant nécessaire**	**33511**	A
Epaisseur cond. retour	8.8	mm	Valeur efficace du courant	1261	A
Hauteur de conducteur retour	60.4	mm	densité de courant eff.	4.27	A/mm2
Résistivité du cuivre (1.72E-2	0.0172	mO.mm	**Résistance de l'aimant**	**0.064**	mOhms
module d'Elasticité (12500	12500	daN/mm2	**Inductance de l'aimant**	**1.27**	uH
Forme de l'impulsion			**Puissance dissipée**	**0.102**	kW
DC , 1/2 sinus : S , trapèze : T	S		Energie stockée	713	J
1/2 période de l'impulsion	3.4	ms			
Période de récurence (cycle tot.	1.2	s			
taux de répétition de l'impulsion de courant					
Systeme de refroidissement				116	p en mm
pression différentielle	12	bar		60.4	h en mm
nombre du circuits	2			189.5	L en mm
septum				207.4	H en mm
forme element de refroidissement	rec				
Cote horizontal	5	mm			
Cote vertical	30.2	mm			
forme du passage d'eau	circ		Débit d'eau total	5.55	l/min
Diametre trou	2	mm	Débit dans chaque spire	2.78	l/min
			vitesse de l'eau dans septum	14.73	m/s
conducteur retour			dT total d'eau	0.29	K
forme element de refroidissement	rec				
Cote horizontal (mm)	8.8	mm	**Force septum /cond fond**	**654.20**	daN
Cote vertical (mm)	30.2	mm	Flèche max . septum (appui	0.026	mm
forme du passage d'eau	rec		moment flech.max. (appui	8.82	mm*daN
Cote horizontal	3.6	mm	contrainte maxi <5 (appui	2.12	daN/mm2
Cote vertical	2.2	mm	Masse culasse (sans poutre	130	kg
Matiere			section cond. septum	295.7168147	mm2
maximum admissible champ dans le f	1.1	T	Section refroidissement septur	6.283185307	mm2

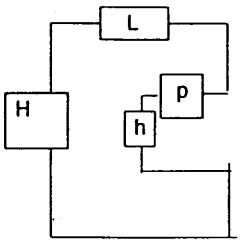

M.THIVENT Version 12 Mai 1992 Edition du : 30.Jun.95

Modifie R, L pour monospire, hydraulique revise 2/8/94 J. Borburgh

PREDETERMINATION SEPTUM MAGNETIQUE SMCALC.XLS **PW prot:jb**

PISMH 42 version ION PLOMB

particularités

DONNEES		
particules electrons : e protons : p	p	
quant.mouvt : MV Energie cin. : EC	ec	
Energie cinétique Ec =	1	GeV
Déflexion requise	54.66	mrad
Epaisseur du septum	5	mm
Hauteur du Gap	60.4	mm
Profondeur du Gap	116	mm
Longueur magnetique equivalent	560	mm
Espace de glissement	0	m
Monospire donc	1	spire
Epaisseur cond. retour	8.8	mm
Hauteur de conducteur retour	60.4	mm
Résistivité du cuivre (1.72E-2	0.0172	mO.mm
module d'Elasticité (12500	12500	daN/mm2
Forme de l'impulsion		
DC , 1/2 sinus : S , trapèze : T	S	
1/2 période de l'impulsion	3.4	ms
Période de récurence (cycle tot.	1.2	s
taux de répétition de l'impulsion de courant		
Systeme de refroidissement		
pression différentielle	12	bar
nombre du circuits	2	
septum		
forme element de refroidissement	rec	
Cote horizontal	5	mm
Cote vertical	30.2	mm
forme du passage d'eau	circ	
Diametre trou	2	mm
conducteur retour		
forme element de refroidissement	rec	
Cote horizontal (mm)	8.8	mm
Cote vertical (mm)	30.2	mm
forme du passage d'eau	rec	
Cote horizontal	3.6	mm
Cote vertical	2.2	mm
Matiere		
maximum admissible champ dans le f	1.1	T

RESULTATS	PROTONS	
Masse au repos mo	0.94	Gev/c2
Energie cinétique	1.0000	GeV
Quantité de mouvement	1.6971	Gev/c
beta	0.8748	
gamma	2.0638	
beta*gamma	1.8054	
Déplact. après espace de gliss	15.3048	mm
Champ intégré B*L	0.309	T.m
Induction dans le Gap	0.552	T
Champ magn. H=B/uo	4.39E+05	A/m
Courant nécessaire	26539	A
Valeur efficace du courant	999	A
densité de courant eff.	3.38	A/mm2
Résistance de l'aimant	0.064	mOhms
Inductance de l'aimant	1.27	uH
Puissance dissipée	0.064	kW
Energie stockée	447	J

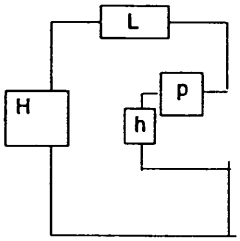

	116	p en mm
	60.4	h en mm
	174.2	L en mm
	176.9	H en mm
Débit d'eau total	5.55	l/min
Débit dans chaque spire	2.78	l/min
vitesse de l'eau dans septum	14.73	m/s
dT total d'eau	0.18	K
Force septum /cond fond	410.30	daN
Flèche max . septum (appui	0.016	mm
moment flech.max. (appui	5.53	mm*daN
contrainte maxi <5 (appui	1.33	daN/mm2
Masse culasse (sans poutre	96	kg
section cond. septum	295.7168147	mm2
Section refroidissement septur	6.283185307	mm2

M.THIVENT Version 12 Mai 1992 Edition du : 30.Jun.95

Modifie R, L pour monospire, hydraulique revise 2/8/94 J. Borburgh

PREDETERMINATION SEPTUM MAGNETIQUE SMCALC.XLS **PW prot:jb**

PISMH 42 version ION PLOMB

particularités

DONNEES			RESULTATS PROTONS		
particules electrons : e protons : p	p		Masse au repos mo	0.94	Gev/c2
quant.mouvt : MV Energie cin. : EC	ec		**Energie cinétique**	**0.8000**	GeV
			Quantité de mouvement	**1.4642**	Gev/c
Energie cinétique Ec =	**0.8**	GeV	beta	0.8415	
			gamma	1.8511	
Déflexion requise	**54.66**	mrad	beta*gamma	1.5577	
Epaisseur du septum	**5**	mm	Déplact. après espace de gliss	15.3048	mm
Hauteur du Gap	**60.4**	mm			
Profondeur du Gap	**116**	mm	**Champ intégré B*L**	**0.267**	T.m
Longueur magnetique equivalent	**560**	mm	**Induction dans le Gap**	**0.476**	T
Espace de glissement	0	m	Champ magn. H=B/uo	3.79E+05	A/m
Monospire donc	**1**	spire	**Courant nécessaire**	**22898**	A
Epaisseur cond. retour	8.8	mm	Valeur efficace du courant	862	A
Hauteur de conducteur retour	60.4	mm	densité de courant eff.	**2.91**	A/mm2
Résistivité du cuivre (1.72E-2	0.0172	mO.mm	**Résistance de l'aimant**	**0.064**	mOhms
module d'Elasticité (12500	12500	daN/mm2	**Inductance de l'aimant**	**1.27**	uH
Forme de l'impulsion			**Puissance dissipée**	**0.048**	kW
DC , 1/2 sinus : S , trapèze : T	S		Energie stockée	333	J
1/2 période de l'impulsion	**3.4**	ms			
Période de récurence (cycle tot.	**1.2**	s			
taux de répétition de l'impulsion de courant					
Systeme de refroidissement				116	p en mm
pression différentielle	**12**	bar		60.4	h en mm
nombre du circuits	**2**			166.2	L en mm
septum				160.9	H en mm
forme element de refroidissement	**rec**				
Cote horizontal	**5**	mm			
Cote vertical	**30.2**	mm			
forme du passage d'eau	**circ**		Débit d'eau total	**5.55**	l/min
Diametre trou	**2**	mm	Débit dans chaque spire	2.78	l/min
			vitesse de l'eau dans septum	14.73	m/s
conducteur retour			dT total d'eau	0.14	K
forme element de refroidissement	**rec**				
Cote horizontal (mm)	**8.8**	mm	**Force septum /cond fond**	**305.44**	daN
Cote vertical (mm)	**30.2**	mm	Flèche max . septum (appui	0.012	mm
forme du passage d'eau	**rec**		moment flech.max. (appui	4.12	mm*daN
Cote horizontal	**3.6**	mm	contrainte maxi <5 (appui	0.99	daN/mm2
Cote vertical	**2.2**	mm	Masse culasse (sans poutre	**79**	**kg**
Matiere			section cond. septum	295.7168147	mm2
maximum admissible champ dans le f	**1.1**	T	Section refroidissement septur	6.283185307	mm2

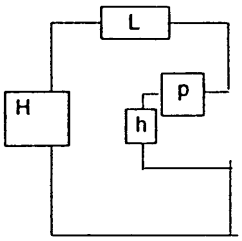

Distribution:

M. Martini
J.P. Riunaud
C. Steinbach
Section PS/ PA/ Septa